occurs in the chirped structure. The applications identified in [2, 3] are examples of the latter. Mizrahi *et al.* have reported an impressive set of results on gratings formed in deuterated, high-germania, erbium-doped fibre [10], including a reflection bandwidth of 10nm with >99% reflectivity. However, their results were obtained for gratings of uniform period, without extrinsic chirp. So far as we are aware, the result represented by Fig. 3 herein represents the largest bandwidth reported from an extrinsically chirped grating of reflectivity as high as 99%.

Conclusions: We have described a method for the fabrication of chirped gratings in photosensitive fibres which is particularly simple insofar as it uses an identical holographic exposure arrangement as for uniform gratings. Experimental verification of the method using boron/germania and hydrogenated germania fibres has been described, resulting in chirped gratings with useful reflectivity/bandwidth combinations not previously reported. We anticipate that the simplicity of the method will prove to be attractive for chirped grating fabrication for many applications which have already been identified.

Acknowledgment: This work was carried out with the support of the SERC under the LINK project GIFTS. We acknowledge our partners in this project, BNR Europe Ltd for supply of the fibres and GEC-Marconi Materials Technology Ltd for assistance with the hydrogenation.

© IEE 1994
4 January 1994

Electronics Letters Online No: 19940276

K. Sugden, I. Bennion, A. Molony and N. J. Copner (*Department of Electronic Engineering & Applied Physics, Aston University, Aston Triangle, Birmingham B4 7ET, United Kingdom*)

N. J. Copner is now with DRA Malvern, St Andrews Road, Great Malvern, Worcs, United Kingdom

References

1 MELTZ, G., MOREY, W.W., and GLENN, W.H.: 'Formation of Bragg gratings in optical fibre by a transverse holographic method', *Opt. Lett.*, 1989, **14**, pp. 823–825

2 OUELLETTE, F.: 'All-fibre filter for efficient dispersion compensation', *Opt. Lett.*, 1991, **16**, pp. 303–305

3 MORTON, P.A., MIZRAHI, V., ANDREKSON, P.A., TANBUN-EK, T., LOGAN, R.A., LEMAIRE, P., COBLENTZ, D.L., SERGENT, A.M., WECHT, K.W., and SCIORTINO, P.F.: 'Mode-locked hybrid soliton pulse source with extremely wide operating frequency range', *IEEE Photonics Technol. Lett.*, 1993, **5**, pp. 28–31

4 MOREY, W.W., DUNPHY, J.R., and MELTZ, G.: 'Multiplexed fibre Bragg grating sensors'. Proc. Distributed and Multiplexed Fibre Optic Sensors SPIE, Vol 1586, Boston, September 1991, pp. 216–224

5 FARRIES, M.C., RAGDALE, C.M., and REID, D.C.J.: 'Broadband chirped fibre Bragg filters for pump rejection and recycling in erbium doped fibre amplifiers', *Electron. Lett.*, 1992, **28**, pp. 487–489

6 BYRON, K.C., SUGDEN, K., BRICHENO, T., and BENNION, I.: 'Fabrication of chirped Bragg gratings in photosensitive fibre', *Electron. Lett.*, 1993, **29**, pp. 1659–1650

7 KASHYAP, R., ARMITAGE, J.R., WYATT, R., DAVEY, S.T., and WILLIAMS, D.L.: 'All-fibre narrowband reflection gratings at 1500nm', *Electron. Lett.*, 1990, **26**, pp. 730–732

8 WILLIAMS, D.L., AINSLIE, B.J., ARMITAGE, J.R., KASHYAP, R., and CAMPBELL, R.: 'Enhanced UV photosensitivity in boron codoped germanosilicate fibres', *Electron. Lett.*, 1993, **29**, pp. 45–47

9 LEMAIRE, P.J., ATKINS, R.M., MIZRAHI, V., and REED, W.A.: 'High pressure H_2 loading as a technique for achieving ultrahigh UV photosensitivity and thermal sensitivity in GeO_2 doped optical fibres', *Electron. Lett.*, 1993, **29**, pp. 1191–1193

10 MIZRAHI, V., LEMAIRE, P.J., ERDOGAN, T., REED, W.A., DIGIOVANNI, D.J., and ATKINS, R.M.: 'Ultraviolet laser fabrication of ultrastrong optical fibre gratings and of germania-doped channel waveguides', *Appl. Phys. Lett.*, 1993, **63**, pp. 1727–1729

Effective index drift from molecular hydrogen diffusion in hydrogen-loaded optical fibres and its effect on Bragg grating fabrication

B. Malo, J. Albert, K.O. Hill, F. Bilodeau and D.C. Johnson

Indexing terms: Optical fibres, Gratings in fibres

When hydrogen loading is used to enhance the photosensitivity of silica-based optical waveguides and fibres, the presence of molecular hydrogen dissolved in the glass matrix changes the effective index of propagation of guided optical modes by as much as 0.05%. Real-time monitoring of the reflectivity spectrum of Bragg gratings written in such conditions shows that the centre wavelength follows the changes in hydrogen concentration due to diffusion and reaction with glass defects.

The refractive index of certain types of doped silica can be modified permanently by exposure to light at blue and UV wavelengths (near 488nm and 244nm, respectively) [1]. The amount of index change depends on several factors arising from the composition of the glass or the fabrication methodology [2]. Recently, two techniques have been proposed to enhance the photosensitivity of germanium-doped silica fibres and waveguides: exposure of the material to the flame of an oxygen-hydrogen burner [3] (usually referred to as 'flame brushing'), and hydrogen loading at high pressures and room temperature [4]. In the flame brushing technique, the enhancement in photosensitivity is due to a strong permanent absorption increase in the 242nm 'oxygen deficient centre' absorption band. On the other hand, the mechanism by which hydrogen loading increases the photosensitivity is not clearly determined at the present time because there is no apparent absorption increase near 240nm following loading alone. The strong UV light used in photosensitivity experiments appears to dissociate the hydrogen molecules dissolved in the glass, leading to the formation of Si-OH and/or Ge-OH groups, as well as oxygen-deficient centres and a large permanent refractive index change. Because the hydrogen starts to diffuse out of the fibre immediately following its removal from the pressure chamber, the photosensitivity enhancement is temporary (by contrast with flame brushing), and UV exposure must be carried out reasonably quickly. It is the purpose of this Letter to quantify the transient effective index drifts associated with the mobility of molecular hydrogen.

In our experiments on the spectral response of Bragg gratings written in hydrogen-loaded optical fibres, we have noticed shifts in the centre wavelength of the reflectivity spectrum which could not be accounted for by UV-induced changes in the average index of the fibre [5]. To clarify this phenomenon, we wrote a Bragg grating in a weakly photosensitive fibre (Corning SMF-28) and then loaded it with hydrogen in the usual manner for 18 days at 100atm. Using the formula relating solubility and equilibrium pressure at 100atm [4], we estimate that the saturated fibre contained 1mol% of dissolved molecular hydrogen. On removal of the fibre from the hydrogen chamber, the Bragg grating was remeasured. We found that the centre of the reflectivity spectrum (λ_B) had shifted by $+0.72 \pm 0.02$nm (from 1533.78 to 1534.50nm), due to the presence of the dissolved hydrogen. Another Bragg grating was immediately written in another section of the same fibre (within 1h of the fibre being removed from the hydrogen chamber). In this case, the initial Bragg wavelength is 1535.66nm, mainly because of a higher average index increase. Both Bragg gratings were fabricated with the same phase mask [6] to ensure the exact reproducibility of the physical periodicity of the index modulation. Then, the reflectivity spectrum of both gratings was monitored over a period of several days.

The centre wavelength of the grating written before hydrogenation decreased gradually over a period of 14 days, eventually reaching the position it occupied immediately after writing. On the other hand, the centre of the reflection spectrum of the grating written after hydrogen-loading shifted to longer wavelengths for about 5h after the UV exposure, and then started to drift back in the other direction. After 14 days, λ_B ended up shorter by -0.16nm than the value measured immediately after writing.

We explain these results in the following manner:

(i) For the case of the grating written prior to hydrogen loading, the presence of the dissolved H_2 in the core of the fibre increases its refractive index by 0.05% (using $\Delta n/n \simeq \Delta\lambda_B/\lambda_B$). Then, as the hydrogen diffuses out, the refractive index returns to its initial value.

(ii) For the grating written immediately after loading, the exposure of the fibre to UV light causes a dissociation of the hydrogen molecules which then react with germanium-associated defects to form Ge-OH bonds. This reaction occurs only in the core of the fibre even though the H_2 molecules dissociate everywhere [4]. In the absence of reaction sites in the cladding, the dissociated molecules most likely recombine. Therefore, immediately after exposure, the core of the fibre is freed of most of the molecular hydrogen, and its refractive index takes a value close to that of a fibre without hydrogen. The cladding is still fully loaded, however, and molecular diffusion occurs to restore equilibrium both towards the core and the outer boundary. During the initial period of 'refilling' of the 4μm-radius core with molecular hydrogen (about 5h) the refractive index increases. Over a longer time period, however, the outer interface at zero hydrogen concentration eventually allows all the remaining hydrogen to escape and the refractive index returns to its 'empty' value. It turns out that the final value of λ_B is blue shifted (by 0.16nm) relative to the original as-written grating, indicating that the core was not completely empty of hydrogen immediately after writing.

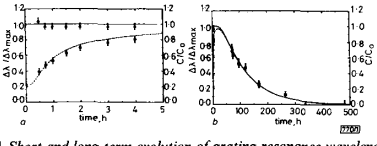

Fig. 1 *Short and long-term evolution of grating resonance wavelength λ_B and of normalised molecular hydrogen C/C_0*

a Short-term evolution
b Long-term evolution

——— $C(H_2)$ for uniform loading
– – – – $C(H_2)$ for UV depleted core
Δ λ_B drift for uniform loading
O λ_B for UV depleted core

This hypothesis has been supported by a simulation of the diffusion of molecular hydrogen using standard Fickian diffusion equations in a cylindrical geometry [7], and assuming that the wavelength shift is roughly proportional to the molecular hydrogen concentration in the centre of the core. For case (i), a single cylinder of diameter equal to the cladding diameter (125μm) is used, with uniform initial concentration C_0 and outer boundary condition set at zero concentration. For case (ii), the initial concentration is zero at the outer cladding boundary, uniform and equal to C_0 in the cladding, and set to a uniform value of 0.16/0.72 $\times$ C_0 in the core (this is a fit of the data to reflect the fact that the core is not fully depleted of molecular hydrogen after the UV exposure, 0.72 representing the maximum λ_B shift corresponding to a concentration C_0 as in case (i), and 0.16 to the difference in λ_B between the as-written grating and the grating with a 'really empty' core concentration obtained after 14 days of out-diffusion). The diffusion coefficient of molecular hydrogen in the fibre is the only free parameter of the simulation and was chosen to fit the model with the experimental data. The results of the simulation are shown in Fig. 1. We see that both short-term and long-term shifts in resonance wavelength are well correlated with the normalised concentration of molecular hydrogen at the centre of the core. The best fit was obtained with a diffusion coefficient of 7.5μm²/h, in good agreement with accepted values for silica fibres [8]. The wavelength shift associated with the presence of H_2 molecules must not be confused with the room temperature decay of shallow colour centres due to normal thermal detrapping [9]. In the conditions used for our experiments, the maximum expected contribution from colour centre decay to a shift in λ_B is smaller than 0.01nm over the time scale covered.

There are several possible physical mechanisms linking the hydrogen loading to the observed drift. By adding 1mol% of H_2 molecules with a molecular polarisability [10] of 0.8×10^{24}cm³ to the silica, the refractive index should increase by 0.12%, corresponding to an increase in λ_B of +1.8nm (we observe +0.72nm)! On the other hand, the dissolved H_2 exerts a dilating pressure on the fibre just taken out of the loading chamber: this pressure tends to reduce the index through the elasto-optic effect. The stress pattern inside the fibre changes further when the core is depleted of H_2 by the UV-induced reaction. The exact modelling of all these contributions depends on the values of various thermodynamic coefficients. However, the voids of the silica network in which the H_2 molecules are trapped are barely bigger than the size of a molecule, so that there is room for only one molecule per site [11]. In this situation, gas laws (and possibly elastic coefficients) become invalid in a statistical sense. The modelling and data shown in Fig. 1 indicate that the combination of all these effects results in a somewhat linear relationship between core molecular hydrogen concentration and Bragg wavelength drift.

These results show that the resonance wavelength of a fibre Bragg grating monitored in real time during the UV exposure differs from the final stable value by several tenths of nanometres. This is due to the relatively large temporary refractive index change induced by the dissolved molecular hydrogen. It is difficult to compensate for this effect or to predict its magnitude because it depends on several factors, especially the residual concentration of hydrogen at the time of exposure and how much core hydrogen depletion has occurred due to the UV exposure. This drift complicates the reproducibility of the central wavelength of Bragg filters and particularly the UV trimming in real time of the optical path length in more elaborate devices, such as waveguide interferometers [12]. The refractive index drift does not occur with flame brushing because the induced sensitisation is stable at room temperature.

© IEE 1994
18 January 1994
Electronics Letters Online No: 19940274

B. Malo, J. Albert, K. O. Hill, F. Bilodeau and D. C. Johnson
(*Communications Research Centre, PO Box 11490, Station H, Ottawa (ONT) K2H 8S2, Canada*)

References

1 HILL, K.O., FUJII, F., JOHNSON, D.C., and KAWASAKI, B.S.: 'Photosensitivity on optical fiber waveguides: application to reflection filter fabrication', *Appl. Phys. Lett.*, 1978, **32**, pp. 647–649
2 HILL, K.O., MALO, B., BILODEAU, F., and JOHNSON, D.C.: 'Photosensitivity in optical fibres', *Annu. Rev. Mater. Sci.*, 1993, **23**, pp. 125–157
3 BILODEAU, F., MALO, B., ALBERT, J., JOHNSON, D.C., HILL, K.O., HIBINO, Y., ABE, M., and KAWACHI, M.: 'Photosensitization of optical fiber and silica-on-silicon/silica waveguides', *Opt. Lett.*, 1993, **18**, pp. 953–955
4 LEMAIRE, P.J., ATKINS, R.M., MIZRAHI, V., and REED, W.A.: 'High pressure H_2 loading as a technique for achieving ultrahigh UV photosensitivity and thermal sensitivity in GeO_2 doped optical fibres', *Electron. Lett.*, 1993, **29**, pp. 1191–1193
5 FERTAIN, E., LEGOUBIN, S., DOUAY, M., CANON, S., BERNAGE, P., NIAY, P., BAYON, F., and GEORGES, T.: 'Shifts in resonance wavelengths of Bragg gratings during writing or bleaching experiments by UV illumination within germanosilicate optical fibre', *Electron. Lett.*, 1991, **27**, pp. 1838–1839
6 HILL, K.O., MALO, B., BILODEAU, F., JOHNSON, D.C., and ALBERT, J.: 'Bragg gratings fabricated in monomode photosensitive optical fiber by UV exposure through a phase mask', *Appl. Phys. Lett.*, 1993, **62**, pp. 1035–1037
7 CRANK, J.: 'The mathematics of diffusion' (Oxford, 1956)
8 LEMAIRE, P.J.: 'Reliability of optical fibers exposed to hydrogen: prediction of long-term loss increases', *Opt. Eng.*, 1991, **30**, pp. 780–789
9 DONG, L., ARCHAMBEAULT, J.L., REEKIE, L., RUSSELL, P.ST.J., and PAYNE, D.N.: 'Bragg gratings in Ce^{3+}-doped fibers written by a single excimer pulse', *Opt. Lett.*, 1991, **18**, pp. 861–863
10 MILLER, T.M.: 'Atomic and molecular polarisabilities', *in* 'CRC handbook of chemistry and physics', 69th Edn., 1989, pp. E68–E72
11 HARTWIG, C.M.: 'Raman scattering from hydrogen and deuterium dissolved in silica as a function of pressure', *J. Appl. Phys.*, 1976, **47**, pp. 956–959

12 BILODEAU, F., HILL, K.O., MALO, B., JOHNSON, D.C., and ALBERT, J.: 'High-return-loss narrowband all-fiber bandpass Bragg transmission filter', to be published in *Photonics. Technol. Lett.*, 1994, **6**

Mixing and detection of microwave signals in fibre-optic electrostrictive sensor

S.T. Vohra and L. Fabiny

Indexing terms: Piezoelectric devices, Fibre optic sensors, Microwave techniques

The nonlinear strain–polarisation relationship in electrostrictive ceramics is exploited to demonstrate, for the first time, detection and mixing of microwave signals in a fibre-optic electrostrictive sensor. The nonlinear electrostrictive transducer mixes the microwave signal with a signal from a local oscillator, and the resulting strain at the intermediate frequency is detected with a fibre-optic interferometer. The sensor demonstrated approximately flat response in the microwave regime (up to 20GHz) with a resolution of 5×10^{-6} V/√Hz.

Electrostrictive ceramics are finding increasing use in a variety of applications including deformable mirrors, positioners, electro-optic shutters and as transducers in high-resolution fibre-optic (FO) voltage sensors. Electrostrictive ceramics differ from piezoelectric ceramics in many respects, especially in their strain–polarisation (electric-field) relationship. While the induced strain in piezoelectric materials is linearly proportional to the applied field, electrostrictive ceramics have a nonlinear strain/electric-field relationship which can be written as $e = ME^2$, where e is the induced strain in the material, E is the applied electric field and M is a frequency-dependent effective electrostriction parameter. The nonlinear strain/electric-field relationship has been exploited to demonstrate a variety of novel devices [1]. For instance, FO voltage sensors employing electrostrictive ceramics have demonstrated high-resolution detection of voltages both at low frequencies (< 1Hz) using a high-frequency dither field [2, 3], and at frequencies in the range 1 – 60kHz using a DC bias field [4]. In this work, the nonlinear strain/electric-field relationship in a lead magnesium niobate (PMN) based electrostrictive transducer is exploited for the first time to demonstrate mixing and detection of microwave signals at frequencies up to 20GHz.

Consider two AC electrical signals applied to the transducer, $E_1\cos\omega_1 t$ and $E_2\cos\omega_2 t$. The fields will generate strain $e = M(E_1\cos\omega_1 t + E_2\cos\omega_2 t)^2$ in the electrostrictor, thus providing strain responses at ω_1, $2\omega_1$, ω_2, $2\omega_2$ and $(\omega_1 \pm \omega_2)$. Owing to the mechanical nature of the effect, significant electrostriction is limited to frequencies below approximately 100kHz [4]. We show in this work that the individual frequencies ω_1 and ω_2 are not restricted to the range of frequencies below 100kHz and can be extended considerably above the range where electrostriction occurs. In other words, to obtain strain at $(\omega_1 - \omega_2)$ it is not necessary to respond electrostrictively at ω_1 and ω_2 ; it is only necessary for the external fields $E_1\cos\omega_1 t$ and $E_2\cos\omega_2 t$ to induce polarisation at ω_1 and ω_2 for mixing to occur. We show that this effect can be successfully exploited to demonstrate a novel type of microwave mixer/detector using fibre-optic interferometry. A similar technique has been used previously to demonstrate mixing and detection of RF magnetic signals (f < 10MHz) in a magnetostrictive transducer [5].

For an electrostrictive transducer driven by two AC electrical signals $E_1\cos\omega_1 t$ and $E_2\cos\omega_2 t$, the strain response at the sum and difference frequencies $(\omega_1 \pm \omega_2)$ can be written as

$$e_{(\omega 1 \pm \omega 2)} = M_{(\omega 1 \pm \omega 2)}(E_1 E_2 \cos(\omega 1 \pm \omega 2)t) \quad (1)$$

where $M_{(\omega_1 \pm \omega_2)}$ is the value of M at frequency $(\omega_1 \pm \omega_2)$. One of the fields $(E_1\cos\omega_1 t)$ can be regarded as the 'test' signal while the second field $(E_2\cos\omega_2 t)$ can be regarded as a local oscillator (LO) whose frequency is tuned to maintain the desired intermediate frequency (IF), $\omega_{IF} = (\omega_1 - \omega_2)$. The sensor effectively acts as a heterodyne detection system where the electrostrictive transducer functions as both the receiving element and the nonlinear mixing element. The resulting strain at IF is detected with a fibre-optic interferometer. Considering only the difference term, the optical phase shift at the IF induced in the optical fibre attached to the electrostrictive transducer is given by

$$\phi_{(\omega 1 - \omega 2)} = (2\pi n\xi/\lambda)LM_{(\omega 1 - \omega 2)}E_1E_2[\cos(\omega 1 - \omega 2)t] \quad (2)$$

where L is the length of the fibre interacting with the transducer, n (= 1.5) is the refractive index of the fibre core, λ is the free space wavelength of the light, and ξ (= 0.78) is the strain-optic factor.

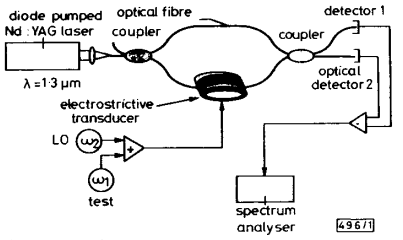

Fig. 1 *Experimental apparatus for mixing experiment*

The experimental arrangement is shown in Fig. 1. A lead titanate (PT) doped lead magnesium niobate (PMN) actuator stack, $(PT)_{0.075}$:$(PMN)_{0.925}$, placed inside an elliptically shaped aluminum shell, forms the electrostrictive transducer. Singlemode optical fibre is wrapped (L = 35m) around the transducer and the assembly incorporated into a fibre Mach–Zehnder interferometer operating at λ = 1.3μm. The sensor employed active homodyne demodulation with a PZT element (not shown) in the reference arm. The electrostrictive coefficient at the IF, which was chosen to be 23.2kHz due to a large mechanical resonance in the transducer at that frequency, was measured to be $M_{(\omega 1 - \omega 2)} = 3.3 \times 10^{-15}$ (m²/V²). The layer thickness (T) of the electrostrictive actuator was 100μm [3]. The test and the LO microwave signals from two microwave synthesisers (HP 8341A) were combined with a conventional microwave combiner and applied directly to the electrostrictive transducer. Although eleetrostrictive materials are capable of responding well above 20GHz, we were limited in our experiments to less than 20GHz due to equipment limitations.

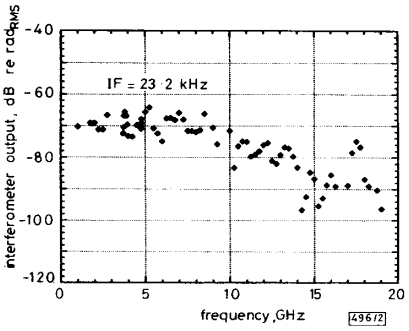

Fig. 2 *Amplitude of strain at difference frequency as function of test signal frequency for IF = 23.2kHz*

Fig. 2 is the interferometer response at the IF frequency, 23.2 kHz, as a function of test signal frequency $\omega_1/2\pi$. The LO frequency was automatically adjusted at each point to maintain $\omega_{IF} = (\omega_1 - \omega_2)$. The response at the IF is shown in terms of the optical phase shift and appears to be flat between 1 and 10GHz. For $(\omega_1/2\pi) \geq$ 10GHz the response tends to show a slight downward slope. This is most likely due to microwave losses in the material as well as sundry parasitic effects at high frequencies. The electrical design of the electrostrictive transducer was not optimised for carrying microwave signals which resulted in microwave losses at higher